Langmuir

ARTICLE

pubs.acs.org/Langmuir

Nanoscale Patterning of Solid-Supported Membranes by Integrated Diffusion Barriers

Mathieu Jung,[†,‡] Nicolas Vogel,[†] and Ingo Köper*[,†,§]

[†]Max-Planck-Institute for Polymer Research, Ackermannweg 10, 55128 Mainz, Germany

[§]Flinders Centre for NanoScale Science and Technology, School of Chemical and Physical Sciences, Flinders University, GPO Box 2100, Adelaide SA 5001, Australia

Supporting Information

ABSTRACT: Ultraflat nanostructured substrates have been used as a template to create patterned solid-supported bilayer membranes with polymerizable tethered lipids acting as diffusion barriers. Patterns in the size range of 100 nm were successfully produced and characterized. The diffusion barriers were embedded directly into the phospholipid bilayer and could be used to control the fluidity of the membrane as well as to construct isolated membrane corrals. By using nanosphere lithography to structure the templates it was possible to systematically adjust the lipid diffusion coefficients in a range comparable to those observed in cellular membranes. Single colloids applied as mask in the patterning process yielded substrates for creation of isolated fluid membrane patches corralled by diffusion barriers. Numerous potential applications for this new model system can be envisioned, ranging from the study of cellular interactions or of molecular diffusion in confined geometries to biosensor arrays.

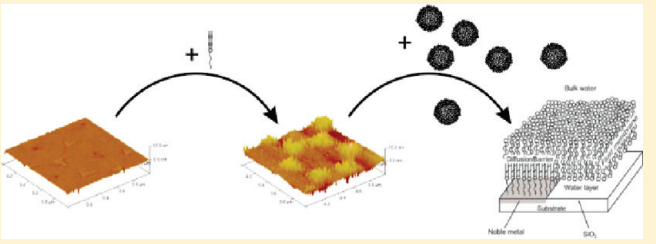

INTRODUCTION

Lipid bilayer model systems that mimic cellular environments have been successfully introduced in the biophysical and medical sciences and have made a significant impact toward the understanding of processes occurring at cell interfaces.[1,2] Numerous commercial and scientific applications have been envisioned, where nonbiocompatible planar devices such as CMOS- or FET-based sensors, noble metals, or microfluidic systems have been functionalized with a plasma-membrane-like coating.[3−6] Such platforms have been used, for example, in the study of cell−cell interactions and communications[7,8] or the design of stable and sensitive biosensing devices based on selective molecular recognition events.[9]

A suitable model membrane system significantly reduces the complexity of a natural membrane and at the same time preserves its main functionalities.[1] Among a wide range of model architectures, solid-supported bilayer lipid membranes have attracted special interest. First, membranes were obtained by direct spreading of amphiphiles on hydrophilic surfaces,[10] subsequently forming two-dimensional, self-assembled fluid systems, separated from the solid substrate by a thin water layer.[11] These systems are perfectly suited to study intrinsic membrane properties; however, they face problems when used to probe incorporated membrane proteins. Most integral proteins involved in metabolic processes, as well as channel proteins widely used for the construction of next generation biosensors,[12,13] are spanning the plasma membrane and protrude into the extra- and intracellular space. A solid-supported model system has thus to provide sufficient space between membrane and substrate in order to allow for protein functionality and to avoid protein denaturation. Various approaches have been developed, ensuring an effective decoupling of the artificial membrane from the substrate. For example, tethered lipid bilayer membranes (tBLMs) utilize synthetic anchor lipids as part of the bilayer, linking membrane and substrate via a spacer unit functionalized with a specific surface binding group.[14] Attachment of thiol or silane moieties to the tether lipids allow for the assembly of membranes on gold or oxide surfaces, respectively.[9,15] These membranes feature superior stability compared to standard solid-supported membranes.[16] Functional incorporation of membrane proteins such as α-Hemolysin and other ion channel proteins has been demonstrated.[17,18]

For a wide range of applications, for example, for the creation of protein or membrane arrays, it would be interesting to selectively control the diffusion of lipids or incorporated membrane proteins within the two-dimensional plane of the membrane by compartmentalization of the artificial bilayer.[19−21] Periodically structured supported membranes[22−31] have been produced by using (photo)polymerizable lipids as part of the membrane for in situ formation of diffusion barriers or by using prestructured substrates. In the latter case, metals, photoresists, or immobilized proteins have been used as barriers while the substrate itself has been functionalized with a lipid bilayer and potentially an

Received: January 5, 2011
Revised: March 20, 2011
Published: April 26, 2011

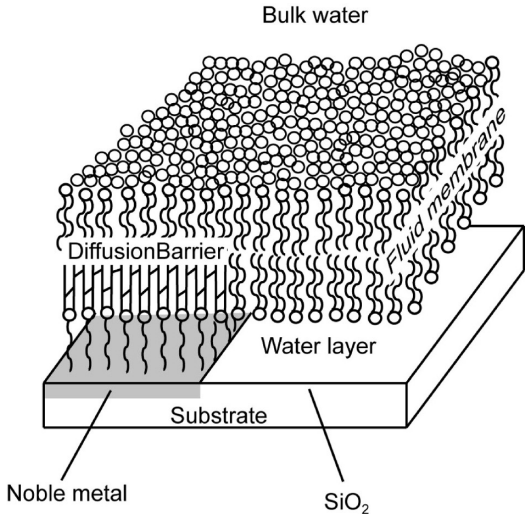

Figure 1. Schematic illustration of a supported membrane, corralled by a self-assembled polymerized lipid barrier. The patterned substrate allows for the controlled assembly of the diffusion barriers embedded into a fluid lipid bilayer membrane.

intermediate cushion layer. The pattern sizes obtained by these methods were typically in the midmicrometer scale, therefore limiting potential applications, e.g., systematic investigation of processes occurring in biological membranes in relation to the cytoskeleton as a natural diffusion barrier. A periodic patterning on the nanoscale remains challenging, as the majority of the proposed procedures involve a photolithographic step in the course of the patterning process.

Here, we present a novel approach to create patterned membrane architectures with nanoscale resolution. The process combines the advantages of a tethered membrane platform, namely, decoupling of the bilayer from the substrate and creation of an ionic reservoir underneath the bilayer with the possibilities offered by introduction of barriers of precise size and spacing. Recently developed ultraflat substrates patterned by nanosphere lithography are used as support.[32] The substrates are composed of different materials, i.e., gold and silicon oxide, with no transition steps in between and a mean surface roughness of less than 5 Å. The different materials can be selectively functionalized, for example, for assembly of polymerizable anchor lipids acting as immobile barriers upon UV polymerization. A fluid bilayer membrane can then be completed by vesicle fusion onto the substrate and thus feature diffusion barriers incorporated into the bilayer lipid membrane. (Figure 1)

Compared to existing membrane patterning approaches, this process offers several advantages. First, no photolithographic step is required during the substrate patterning. Thus, the resolution of the diffusion barriers is not limited by the diffraction limit of light, and structure sizes down to 30 nm are created with ease. Furthermore, the immobile fractions are formed by polymerizable lipids and are part of the membrane. They provide therefore stability to the system and allow one to circumvent issues related to undefined lipid bilayer formation at the edges of membrane patches.[33]

Here, the characterization of newly synthesized polymerizable lipids, selective functionalization of nanostructured gold domains using these lipids, and formation and compartmentalization of a fluid membrane are presented. Finally, fluorescence recovery after photobleaching (FRAP) experiments were used to examine lipid diffusion within the resulting patterned membranes. Using colloidal particles as a mask for the substrate prestructuring process, both arrays of nanoscale diffusion barriers as well as isolated fluid membrane patches corralled by diffusion barriers were obtained. The former were used to control the diffusion constants of the lipids over 1 order of magnitude, while the latter effectively captured lipids in the proximal leaflet in the fluid areas.

EXPERIMENTAL SECTION

Materials. All reagents for synthesis were purchased from Sigma-Aldrich (Schnelldorf, Germany) and used without further purification. Solvents were obtained from Fischer Scientific (Niderau, Germany) in HPLC grade and dry solvents from Acros Organics (Niderau, Germany). The purity of the obtained products was controlled by ^{1}H NMR and mass spectrometry. For details on the synthesis procedure of the polymerizable anchor lipids, please refer to the Supporting Information.

Vesicle Fusion. 1,2-Dioleoyl-*sn*-glycero-3-phosphoethanolamine-*N*-(7-nitro-2−1,3-benzoxadiazol-4-yl) (DOPE-NBD) and 1,2-diphytanoyl-*sn*-glycero-3-phosphocholine (DPhyPC) were purchased from Avanti Polar Lipids (Alabaster, AL) and used as received. Small unilamellar vesicles (50 nm in diameter) were prepared by extrusion of a 2 mg/mL lipid solution (DPhyPC and 0.8 mol % DOPE-NBD) in ultrapure water (R > 18 MΩcm, Millipore, Schwalbach, Germany). The vesicles were stored at 4 °C and used within 2 days. Vesicle fusion was performed in 0.1 M KCl solution.

Lipid Self-Assembly. In order to form densely packed monolayers of the polymerizable lipids, two strategies were used. For experiments to pattern a membrane using photolithography on a homogeneous substrate, a Langmuir−Blodgett transfer was performed as described below. Polymerization was achieved by UV illumination at 254 nm at room temperature under N_2 atmosphere using a 6 W laboratory hand lamp at a distance of 5 cm, delivering 5.8 mW/cm^2.

For laterally patterned substrates, a simple self-assembly process was used to form a monolayer selectively on the gold part of the substrates. The polymerizable thiolipids were self-assembled by immersion of the sample in a 0.2 mg/mL ethanolic solution of the lipid for 24 h, followed by thorough rinsing with ethanol.[34,35]

Langmuir Isotherms. Langmuir isotherms were recorded at 20 °C on a KSV Minitrough (KSV Instruments, Helsinki, Finland). Stock solutions of the different anchor lipids in chloroform (2 mg/mL) were used. Isotherms were recorded at a constant compression rate of 5 mm/min. A Langmuir−Blodgett transfer onto a solid substrate was performed with a deposition speed of 1 mm/min at a surface pressure of 50 mN/m.

UV−Vis Spectroscopy. The polymerization kinetics of the silane-based polymerizable anchor lipid (cf. Figure 5, HC2TES) was followed on quartz substrates. Monolayers were transferred from the air−water interface by Langmuir−Blodgett transfer.

In order to determine the polymerization kinetics of the synthesized anchor lipids, UV−vis spectra were recorded in transmission mode from 820 to 220 nm in between different UV irradiation steps (Lambda 900, Perkin-Elmer, Waltham, MA).

Substrates. The heterogeneous substrates were prepared using a multistep procedure based on a template-stripping process (Figure 2).[32,36−38] First, a silicon wafer was coated with an octadecyltriethoxysilane layer, reducing the adhesion between wafer and deposited structures. Subsequently, colloidal particles were deposited onto the substrate to serve as a mask for subsequent gold evaporation. Either sparsely distributed silica beads (2 μm in diameter, Duke Scientific Corp., CA) or densely packed colloidal monolayers were used as masks (Figure 2a). Individual beads were distributed onto the substrate by spin coating from a 0.05 wt % ethanolic solution at 1500 rpm for 60 s, while the monolayers were preassembled onto an air−water interface[39] and transferred onto the silicon substrate. Layers of 50 nm Au and 5 nm

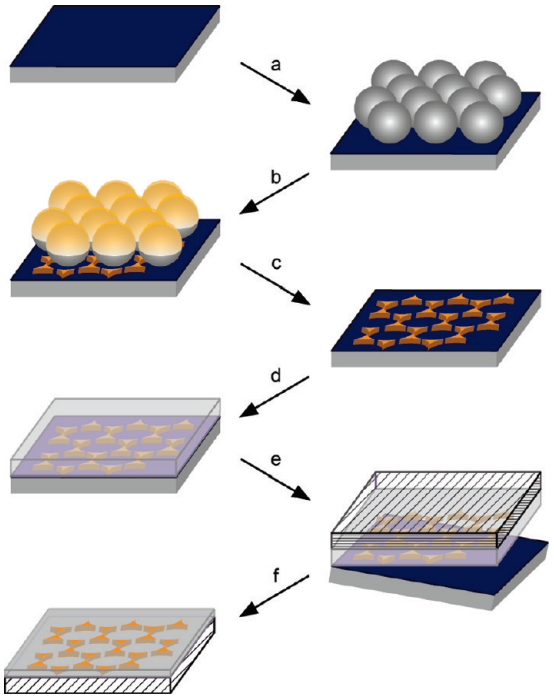

Figure 2. Process flow for fabrication of heterogeneous ultrasmooth patterned substrates. (a) Assembly colloidal particles onto the silanized silicon wafer. (b) Evaporation of gold (50 nm) and chromium (5 nm). (c) Colloid removal. The areas not protected by the colloids are transferred into gold structures. (d) Evaporation of 100 nm of silicon dioxide onto the complete surface (for all FRAP experiments, an additional layer of gold was evaporated that is omitted for reasons of clarity). (e) Gluing of a glass slide onto the wafer. The created structures are sandwiched between wafer and glass. (e and f) Mechanical separation of the wafer template. The interface between wafer and evaporated structures is thus revealed on the glass slide.

Cr (used to promote adhesion between gold and the subsequently deposited SiO_2 layer) were evaporated onto the substrate. The individual beads or the colloid monolayers were removed from the substrate by intensive rinsing with THF, thus producing gold patterns on the silicon wafer (Figure 2c). Subsequently, 110 nm of SiO_2, 5 nm Cr, and 100 nm Au were deposited (Figure 2d) before the sample was glued to a microscope glass slide with an epoxy resin (Epotek, Billerica, MA). For reasons of clarity, Figure 2d only shows the silicon dioxide evaporated onto the substrate. The subsequent deposition of chromium and gold provide a layer to block fluorescence of the epoxy glue. As it is buried in the substrate, the layer does not affect the topography. The heterogeneous substrate interface, consisting of gold areas embedded in an oxide matrix, was then revealed by mechanical separation of the passivated silicon wafer template from the microscope slide (Figure 2e). The low surface roughness of the wafer surface is thus transferred to the heterogeneously patterned surface, featuring nanostructures of one material embedded in the other without any gaps or surface topography between them (cf. Figure 7). Using a colloid monolayer as a shadow mask led to hexagonally packed gold nanotriangles embedded in an oxide matrix, while the single colloids gave rise to individual SiO_2 patches in a continuous gold film (compare Supporting Information). The substrates were then used to introduce immobile obstacles in the solid-supported membrane by self-assembly of the polymerizable lipids.

AFM. Atomic force microscopy images were obtained on a Dimension 3100 microscope (Veeco Instruments, Plainview, USA) with Nanoscope version 7.20 software. The silicon cantilevers used for the measurements had a resonance frequency of 300 kHz (Olympus, Tokyo, Japan).

Fluorescence Recovery after Photobleaching. FRAP experiments were performed using a customized setup based on an Olympus IX70 inverted microscope equipped with a photomultiplier (Type B2F/RFI, Electron Tubes Ltd., Middex, U.K.).[40] The samples were illuminated with a mercury lamp integrated in the microscope for observation and focusing, whereas the FRAP measurements were performed with the 488 nm line of an argon ion laser, creating a circular spot (Ø 4.2 μm). All measurements were conducted at room temperature in PBS buffer and repeated at least 15 times for each membrane.

Diffusion coefficients were determined by adjusting the experimental data to a model developed by Soumpasis[41,42]

$$f_k(t) = F_k(\infty) - [F_k(\infty) - F_k(0)] \cdot \left\{1 - \exp\left(\frac{-\omega^2}{2Dt}\right) \cdot \left[I_0\left(\frac{\omega^2}{2Dt}\right) + I_1\left(\frac{\omega^2}{2Dt}\right)\right]\right\}$$

where ω is the radius of the bleaching spot, t is the time, $F_k(0)$ is the minimum fluorescence intensity after photobleaching, $f_k(t)$ is the fluorescence intensity at time t, $F_k(\infty)$ is the fluorescence intensity as t reaches ∞, I_0 and I_t are spherical Bessel functions of zero and first order, and D is the diffusion coefficient.

The relative recovery, indicating the fraction of mobile lipids within the measured leaflet, is defined as

$$\text{relative recovery} = \frac{F_\infty - F_0}{F_- - F_0} \cdot 100\%$$

where F_- is the fluorescence intensity before bleaching, F_0 is the fluorescence immediately after bleaching, and F_∞ is the recovered fluorescence intensity.

RESULTS AND DISCUSSION

Anchor Lipids. The synthesized anchor lipids were composed of three parts, i.e., a hydrophobic moiety that inserted into the bilayer, a short spacer decoupling the membrane from the substrate, and a surface-specific anchor group (Figure 3).[9,43]

The alkyl chains of the hydrophobic part were modified with diacetylene groups, which enables the cross-linking of the proximal leaflet of the membrane to form diffusion barriers upon polymerization.[26] Long fatty acid chains with diacetylene groups were chosen in order to allow for the formation of a light-sensitive crystal with the ability to polymerize at room temperature.

The selective polymerization of lipids was first introduced to enhance the long-term stability of liposomes[44−48] or bilayer lipid membranes.[49,50] Different classes of polymerizable lipids have been used in the past, mostly based on acrylate or diacetylene derivatives. These polymerizable units were mainly located in the hydrophobic chains.[46,47,50−52] Since diacetylene derivates polymerize under topochemical conditions, they require a high packing order of the reactive groups in a lattice.[53] The polymerization then yields a rigid, conjugated polymer backbone, which is expected to form impermeable diffusion barriers within a membrane.

For the selective functionalization of the noble metal or oxide areas of the patterned substrate, lipids with specific surface binding groups were synthesized; namely dithiolane functionalized lipids for gold surfaces and triethoxysilane lipids for oxide or nitride surfaces. The self-assembly of the thiolipids from an ethanolic solution was demonstrated by the specific functionalization of the gold regions of the patterned substrate (cf. Figure 7).

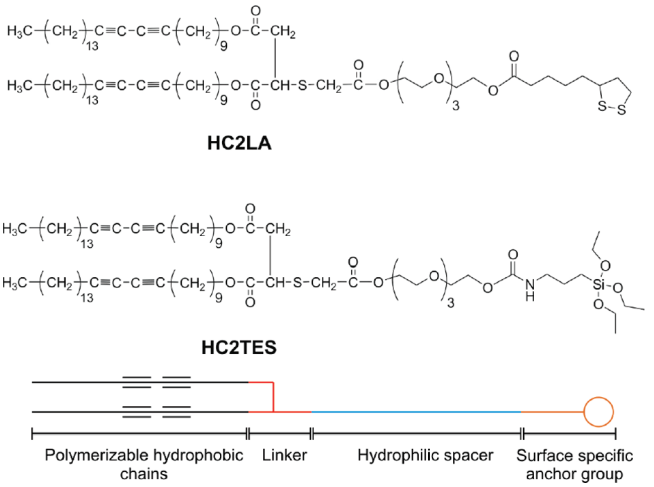

Figure 3. Chemical structures of the polymerizable anchor lipids HC2LA and HC2TES. For details about the synthesis, please refer to the Supporting Information.

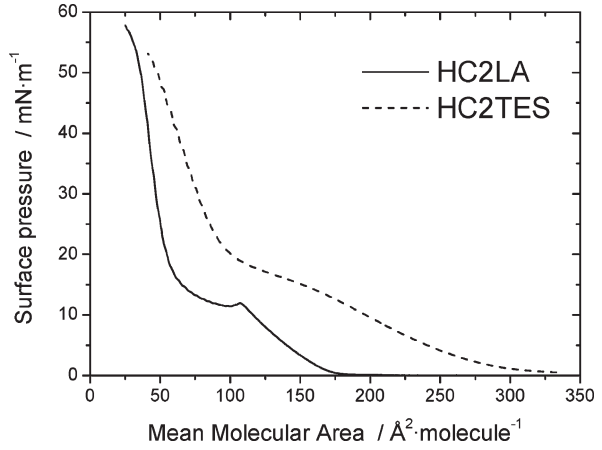

Figure 4. Langmuir pressure−area isotherms of the anchor lipids measured at 20 °C.

A short poly(ethylene glycol) (PEG) chain was used as a spacer in all molecules. The ethylene oxide repeating units as polar, uncharged hydrogen-bond accepting groups undergo multiple bonds with water molecules in aqueous solutions. They thus decouple the membrane from the substrate and can create an ion reservoir underneath the bilayer. Both functions are prerequisites for the functional incorporation of membrane proteins. Additionally, the flexibility of the PEG chains allows them to adapt to membrane fluctuations, preventing ruptures in the bilayer.[54]

Film Properties at the Air−Water Interface. Lipid films at the air−water interface were characterized by Langmuir isotherms, which give information about the interplay of the hydrophobic and hydrophilic parts of the molecules. Diacetylenic amphiphiles are known to form liquid crystalline phases upon compression at the air−water interface. Moreover, polymerization is only possible in these liquid crystalline phases.[55]

The obtained isotherms (Figure 4) showed a typical profile for anchor lipids that form stiff films.[56] Both lipids showed a liquid-expanded phase at higher mean molecular areas, resulting from the interactions of the spacer groups in the subphase. At the onset

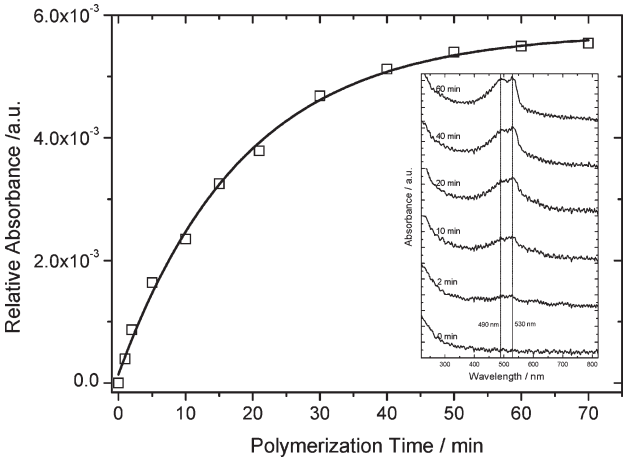

Figure 5. Absorbance of a HC2TES membrane obtained by LB transfer at 50 mN/m measured at 529 nm showed first-order kinetics with a time constant of about 18 min. (Inset) UV−vis spectra at selected time intervals.

of the liquid-expanded to liquid-crystalline transition plateau, an "overshoot transition" was observed for the thiolipids, characteristic for very stiff films.[51,57] Upon further compression of the films, a transition state to liquid-crystalline films was observed, with collapse pressures of 57 mN/m at 22 Å^2/molecule for the thiolipid (HC2LA) and 53 mN/m at 41 Å^2/molecule for the silane lipid (HC2TES). The isotherms were used to determine ideal transfer pressures, which were set at 50 mN/m.

Polymerization of Anchor Lipids. The topochemical polymerization of diacetylenes results in a conjugated backbone of alternating double and triple bonds. These structures exhibit strong absorption bands in the visible spectra of light, which typically leads to a deep blue or deep red coloration of the films. Hence, polymerization of the lipids can be easily followed by UV−vis absorption spectroscopy. Since the lipid monomers do not absorb in the visible range, the polymerization reaction was directly followed as an increase in absorbance (Figure 5). A monolayer of HC2TES was transferred onto a quartz slide at a surface pressure of 50 mN/m and irradiated by UV light, and UV−vis spectra were recorded as a function of the irradiation time. The characteristic peaks of polydiacetylene films at 490 and 529 nm appeared with increasing UV polymerization time.[46,50,51,53,58] The formation of blue intermediate species, absorbing around 620−630 nm, was not observed.[56] The absorption at 529 nm increased exponentially with a time constant of τ = 18 min until saturation was reached after 60−70 min of irradiation.

The experiment has been successfully reproduced using HC2LA on ultraflat gold substrates, where the membrane was prepared either by LB transfer or by self-assembly from an ethanolic solution (data not shown). The kinetics indicates that the degree of cross-linking of the polymerizable lipids can be controlled by varying the irradiation time. As the polymerized monolayer was used as a diffusion barrier, polymerization conditions were always chosen as to produce the highest degree of cross-linking.

When illuminated through a photolithographic mask, selected areas of the films were cross-linked and patterns of polymerized and nonpolymerized membranes were formed. The cross-linked parts appeared as bright areas under a fluorescence microscope (Figure 6), easily distinguishable from the non-cross-linked parts.

dx.doi.org/10.1021/la200027e |*Langmuir* 2011, 27, 7008–7015

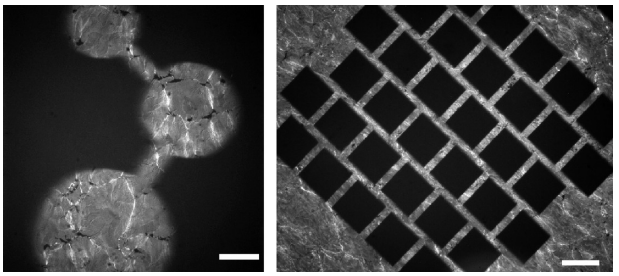

Figure 6. Fluorescence microscope images of patterned lipid membranes on glass (scale bars 100 μm). Anchor lipids were transferred to the substrate by LB transfer and UV-cross-linked through a mask.

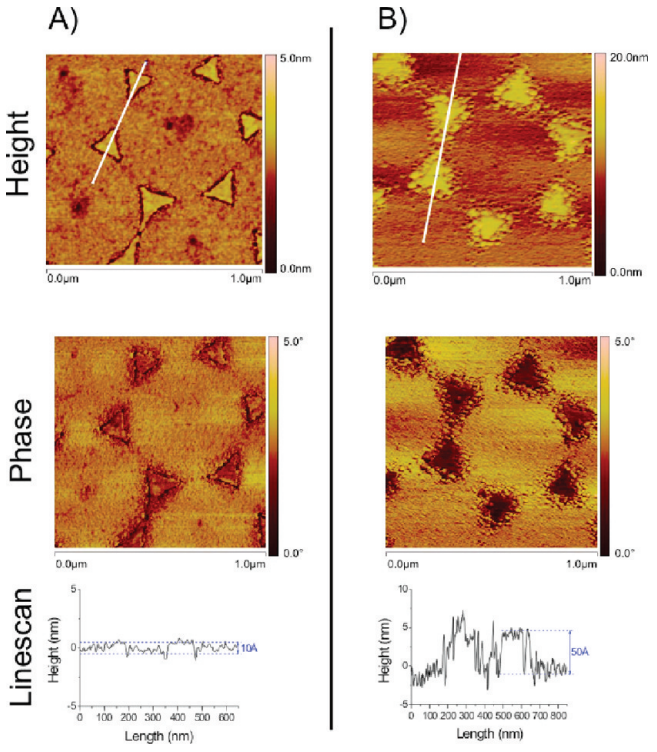

Figure 7. AFM images of patterned substrates and line scan: pristine substrate (A) before self-assembly and (B) after self-assembly.

Photolithography can thus be applied to produce fluid lipid bilayers with incorporated diffusion barriers in microscale dimensions simply by completing the bilayer structure by vesicle fusion, as described below. Furthermore, the polymerization protocol was adapted to polymerize lipids assembled onto the nanoscale barriers as described below in order to ensure a high degree of polymerization.

Paired with the nanoscale patterning technique described below, the Langmuir−Blodgett transfer followed by UV polymerization also would allow for hierarchical patterning of membranes, e.g., by producing large channels of cross-linked lipids that are further structured by nanoscale diffusion barriers. Such structures might prove useful in sophisticated biosensor applications or in the study of complex diffusion phenomena.

Functionalization of the Substrates with the Anchor Lipids. In order to investigate the self-assembly process of the anchor lipids, structured substrates were prepared as described in the Experimental Section using a monolayer of 550 nm

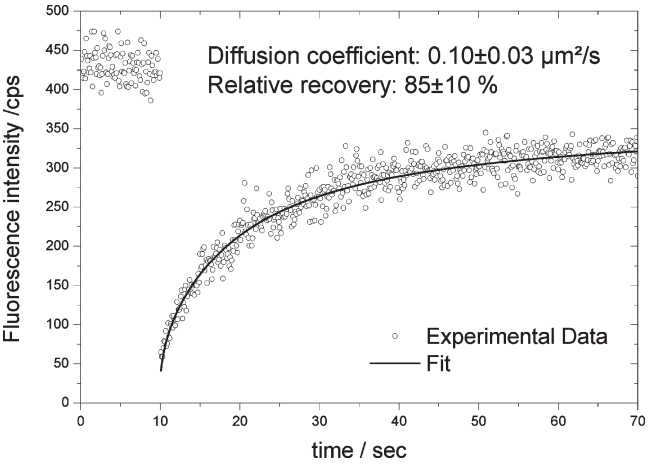

Figure 8. Representative FRAP curve of the artificial membrane prepared on patterned substrates (using 550 nm colloids).

polystyrene colloids as mask. This resulted in the creation of gold nanotriangles embedded in a silicon dioxide matrix.[32,22] The selectivity of the functionalization process was assessed by the comparison of AFM pictures of the gold structures before and after immersion in an ethanolic solution containing the HC2LA lipid.

First, AFM images were recorded directly after the mechanical separation from the silicon wafer and before functionalization (Figure 7A). The phase image clearly shows the material contrast produced by the different hardness of the silicon dioxide and gold areas. The height image and respective line scan highlight the extremely low surface roughness (rms roughness 2 Å) of the substrate. It has been shown that a low surface roughness is essential for the formation of supported membranes with high electrical sealing properties.[35]

The second series of AFM images (Figure 7B) shows the patterned substrates after functionalization. The phase image displayed a higher contrast between the structures and the silicon oxide matrix; a clear difference in height is recorded over the functionalized gold, indicating the presence of the lipid monolayer. The measured height of the monolayer in a dried state of about 50 Å is in good agreement with the calculated persistence length of the HC2LA molecule (60 Å).

The oxide surfaces of the substrates remained clean from lipids or lipid aggregates. However, the triangular shapes were featuring less sharp contours after lipid self-assembly, due to the apparition of satellites of a few nanometers in the vicinity of the main structures. These satellites resulted from the functionalization of small gold residues, deposited next to the main structures, due to diffusion processes occurring during the metal deposition process. These satellites can also be seen in the AFM phase image of the pristine substrate (Figure 7 A). However, as can be seen from the AFM images and the results of the FRAP experiments (Figure 8), the individual lipid-functionalized gold triangles were not interconnected, thus allowing diffusion of free lipids through the barriers.

In contrast to previously published approaches for patterned solid-supported bilayer membranes,[22] the nanoscale diffusion barriers produced by the assembly of the lipids onto surface-embedded nanotriangles gives rise to a patterned membrane system that is not perturbed by the presence of topological features of a different material (e.g., gold). Such elevated barriers

dx.doi.org/10.1021/la200027e |*Langmuir* 2011, 27, 7008–7015

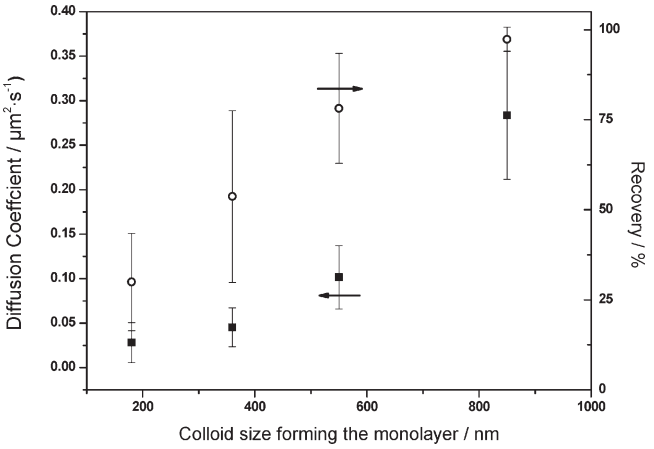

Figure 9. Diffusion coefficients and percentage of recovery as a function of the colloid size used for patterning of the substrate. (squares, left axis: diffusion coefficients; circles, right axis: recovery.

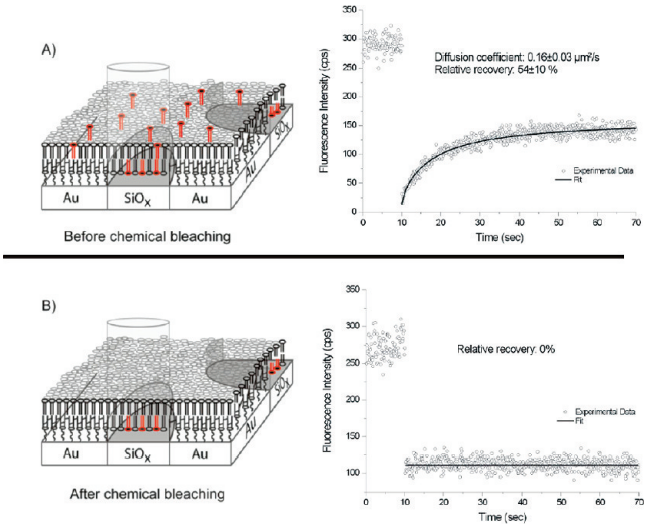

Figure 10. Schematic depiction and measured diffusion curves of FRAP experiments performed on isolated lipid corrals. (A) FRAP experiments to probe diffusion in both leaflets simultaneously. (B) FRAP experiment on the proximal leaflet only.

are known to induce changes in the membrane properties, e.g., through imperfections in the membrane assembly at the edges of the barriers. The here presented system avoids suchs effects by eliminating topographical features in the substrate.[59]

Fluidity of the Artificial Membrane. The previously characterized substrates produced by nanosphere lithography of 550 nm colloids were further used for creation of the patterned model membrane architecture (Figure 1). After functionalization of the substrates, the self-assembled lipids were polymerized by UV irradiation and a bilayer was completed by the fusion of small unilamellar vesicles composed of DPhyPC/DOPE-NBD. In order to probe the fluidity of the obtained bilayers, the lateral diffusion of the lipids was measured by FRAP over the whole substrate (Figure 8).

Since the nanostructures were not interconnected, diffusion of lipids was possible both in the proximal and in the distal leaflets of the membrane. The measured diffusion coefficient of 0.10 ± 0.03 $\mu m^2/s$ was significantly lower than the typical diffusion coefficients of 1−2 $\mu m^2/s$ in solid-supported membranes (see Supporting Information for measurement statistics).[60] This shows that the immobile obstacles had a significant impact on the membrane fluidity. However, the fluorescence recovery of 85% demonstrated that diffusion of the lipids in both leaflets was possible and thus indicated the presence of a complete lipid bilayer architecture. The incomplete fluorescence recovery to the initial level can be partially related to defects in the solid substrate, as discussed in the following set of experiments.

Influence of the Obstacle Lattice and Barrier Size on the Lipid Diffusion Coefficients. The hybrid membrane architecture features barriers in the nanometer regime. Since the size of the diffusion barriers is not limited by the diffraction limit of light, as for the conventional patterning methods, biologically relevant obstacle sizes can be reached, e.g., lipid rafts domains, immobilized protein domains on the cytoskeleton.[61−63]

To explore the effects of the barrier size and obstacle lattice on diffusion within the membrane, the size of the colloids used in the substrate patterning process was varied. As this patterning procedure yields arrays of triangles corresponding to the voids in the colloidal monolayer, the dimensions of the triangular structures can be precisely adjusted by the used colloids. By using colloids of 180, 360, 550, and 850 nm, the immobile obstacles were adjusted to be between 30 and 250 nm. Due to the specific technique of nanosphere lithography, the fraction of immobile obstacles was intrinsically fixed to 9.3%. The diffusion coefficients and fluorescence recovery decreased with decreasing barrier size (Figure 9). This can be attributed to an increase in the number of obstacles per area the lipids have to pass in their diffusion path. By varying the barrier size, it was possible to adjust the mobility of the lipids over 1 order of magnitude from 0.03 ± 0.02 to 0.28 ± 0.07 $\mu m^2/s$. These diffusion coefficients reflect that the membranes with the embedded obstacles had a similar fluidity to cell membranes.[60]

The decrease in the recovery can be for two reasons. First, the amount of defects per area will increase for smaller obstacle sizes, as the size of single-crystalline domains will be reduced for smaller colloids. The influence of defects in the template, which are due to a nonuniform colloid crystal formation during production of the substrate, on the diffusion coefficient was not systematically analyzed. Second and probably more important is that even though the overall fraction of the immobile obstacles remains constant at 9.3%, the contour length of the polymerized lipid islands is increasing for smaller colloids. Freely diffusing phospholipids in the vicinity of the barriers will experience a reduction of their mean free path of diffusion due to the presence of obstacles as impermeable objects as well as due to interactions of the phospholipids with the immobilized anchor lipids. This will lead to an effective increase of the fraction of immobilized lipids in the bilayer. It can be seen that for the largest colloids used, the available area is large enough to allow for almost 100% recovery.

Solid-Supported Membrane Corrals. While periodically patterned, open structures are of interest to study fundamental processes occurring in biological membranes, the confinement of molecules to a defined place in the membrane is of key importance for construction of biosensors. In order to demonstrate the possibility to corral lipids in the proximal leaflet of the membrane by polymerized barriers, substrates with isolated silicon dioxide discs embedded in a gold film were prepared (see Supporting Information for a scheme of the process). Glass beads (2.5 ± 0.5 μm) were used as a mask, and the obtained

dx.doi.org/10.1021/la200027e |*Langmuir* 2011, 27, 7008–7015

structures were thus of about the same size as the laser spot used to bleach the lipids in a FRAP experiment. An AFM investigation of the substrate surface is shown in the Supporting Information. The gold parts of the substrate were functionalized with the polymerized lipids by self-assembly. After fusion of lipid vesicles to complete the hybrid membrane structure, diffusion of the lipids over the oxide islands was measured.

FRAP measurements were performed on both leaflets (Figure 10 A) and on the proximal leaflet only (Figure 10 B). For the latter experiments, the fluorophores in the distal leaflet were chemically bleached by reduction with sodium dithionite.[64] For all experiments, the laser spot was focused onto a single silicon dioxide disk.

Diffusion over both leaflets showed a recovery of approximately 50% (Figure 10 A). Assuming an equal distribution of the fluorescently labeled lipids in both leaflets, this corresponds to an effective prevention of diffusion in the inner leaflet and a closed, fluid outer leaflet spanning both fluid membrane parts and photopolymerized lipids. After the chemical bleaching of the fluorophores in the outer leaflet, the FRAP experiment probed only the diffusion in the inner leaflet. No fluorescence recovery was measured (Figure 10 B), indicating that diffusion of lipids in the proximal leaflet from neighboring corrals was prevented and the polymerized lipids acted as effective diffusion barriers. Eventual flip-flop processes, i.e., transfer of lipids between the inner and the outer leaflet of the membrane, can be excluded due to the much longer time scale on which such processes typically happen.

For the construction of a robust biosensor platform, the introduction of diffusion barriers is a major advantage, as proteins can be confined to a predefined area, e.g., to a single electrode on an array. Furthermore, the sealing properties of the lipid bilayer remain virtually unaffected as the barriers are homogenously incorporated into the fluid membrane as demonstrated by the complete lipid recovery in the distal leaflet.

CONCLUSIONS

An artificial patterned membrane is presented, where tethered immobile obstacles are embedded in the lipid bilayer in a controlled way and on a nanometer scale. The architecture offers a number of attractive features. First, the size of the immobile obstacles is not limited by the diffraction limit. This has been a significant limitation when conventional photolithographic methods have been used for a direct patterning of a photopolymerizable membrane or for the structuring of substrates with diffusion barriers.[27,28,31] By employing nanosphere lithography as a technique to structure the template surface, a precise adjustment of barriers on the nanometer scale is feasible.

Second, the tethered lipids are part of the membrane and thus decouple the bilayer from the substrate. At the same time they act as immobile obstacles. The embodiment of the barriers avoids the problems arising from phase changes observed at the edge of membrane patches.[33]

Finally, utilization of template substrates that have been prepared by a robust replica method ensures preparation of reproducible membrane architectures. As the substrate is flat compared to the anchor lipid dimensions, the molecular diffusion barriers merge homogeneously into the intact bilayer without inducing unwanted effects on the membrane arising from different materials (e.g., photoresist) and edge effects induced by barriers not incorporated into the membrane. Furthermore, while the anchor lipids remain the same, the composition of the bilayer can be changed with ease by varying the lipid mixture of the vesicles.

Patterning of lipid membranes with small dimensions can have various applications. Formation of diffusion barriers in a membrane can be used to study principle diffusion processes in confined geometries in general and in a lipid bilayer in particular. This will enhance the understanding of diffusion barriers as they occur in nature.[60] Additionally, membrane corrals will be useful for immobilization of proteins on biosensing devices.[65] The combination of patterned substrates with photopolymerizable diffusion barriers allows one to selectively localize membrane proteins over certain areas on the substrate, ideally directly over an electrode in a membrane array. However, as this article focuses on the synthesis, assembly, and polymerization of anchor lipids and their application as diffusion barriers with nanoscale dimensions, detailed experiments on biological systems are not in the scope of the study presented here and will be addressed in subsequent publications.

ASSOCIATED CONTENT

Supporting Information. Description of the chemical synthesis of the polymerizable lipids, construction scheme, and AFM images of the substrate patterned with single colloids as mask; FRAP reference measurements. This material is available free of charge via the Internet at http://pubs.acs.org.

AUTHOR INFORMATION

Corresponding Author

*Phone: +61 8 8201 2451. E-mail: ingo.koeper@flinders.edu.au.

Present Addresses

‡IMM GmbH, Carl-Zeiss Strasse 18-20, 55129 Mainz, Germany.

ACKNOWLEDGMENT

Prof. Dr. H. Ringsdorf is gratefully acknowledged for sharing his unique experience on diacetylenes and Dr. M. Retsch for his precious help with colloidal monolayer preparations. The authors further acknowledge Prof. Dr. K. Landfester and Dr. C. Weiss for fruitful discussions. N.V. acknowledges funding from the Materials Science in Mainz (MAINZ) graduate school.

REFERENCES

(1) Chan, Y.-H. M.; Boxer, S. G. *Curr. Opin. Struct. Biol.* **2007**, *11* (6), 581–587.

(2) Vitovic, P.; Kresak, S.; Naumann, R.; Schiller, S. M.; Lewis, R.; McElhaney, R. N.; Hianik, T. *Bioelectrochemistry* **2004**, *63* (1−2), 169–176.

(3) Fertig, N.; Blick, R. H.; Behrends, J. C. *Biophys. J.* **2002**, *82*, 3056–3062.

(4) Albertorio, F.; Diaz, A. J.; Yang, T. L.; Chapa, V. A.; Kataoka, S.; Castellana, E. T.; Cremer, P. S. *Langmuir* **2005**, *21* (16), 7476–7482.

(5) Trojanowicz, M.; Miernik, A. *Electrochim. Acta* **2001**, *46*, 1053–1061.

(6) Mueller, P.; Rudin, D. O.; Tien, H. T.; Wescott, W. C. *Nature* **1962**, *194*, (4832), 979−&.

(7) McConnell, H. M.; Watts, T. H.; Weis, R. M.; Brian, A. A. *Biochim. Biophys. Acta* **1986**, *864* (1), 95–106.

(8) Watts, T. H.; Gaub, H. E.; Mcconnell, H. M. *Nature* **1986**, *320* (6058), 179–181.

(9) Köper, I. *Mol. Biosyst.* **2007**, *3* (10), 651.

(10) Sackmann, E. *Science* **1996**, *271* (5245), 43–48.
(11) Ajo-Franklin, C. M.; Yoshina-Ishii, C.; Boxer, S. G. *Langmuir* **2005**, *21* (11), 4976–4983.
(12) Wu, H.-C.; Astier, Y.; Maglia, G.; Mikhailova, E.; Bayley, H. *J. Am. Chem. Soc.* **2007**, *129* (51), 16142–16148.
(13) Bayley, H. *Nature* **2009**, *459* (7247), 651–652.
(14) Schiller, S. M.; Naumann, R.; Lovejoy, K.; Kunz, H.; Knoll, W. *Angew. Chem., Int. Ed.* **2003**, *42*, (2), 208−+.
(15) Atanasov, V.; Atanasova, P.; Vockenroth, I.; Knorr, N.; Köper, I. *Bioconjugate Chem.* **2006**, *17*, 631–637.
(16) Vockenroth, I. K.; Ohm, C.; Robertson, J. W. F.; McGillivray, D. J.; Lösche, M.; Köper, I. *Biointerphases* **2008**, *3* (2), FA68–FA73.
(17) Vockenroth, I. K.; Atanasova, P. P.; Jenkins, A. T. A.; Koper, I. *Langmuir* **2008**, *24* (2), 496–502.
(18) Vockenroth, I. K.; Atanasova, P. P.; Long, J. R.; Jenkins, A. T. A.; Knoll, W.; Köper, I. *Biochim. Biophys. Acta: Biomembr.* **2007**, *1768* (5), 1114–1120.
(19) Rodgers, W.; Zavzavadjian, J. *Exp. Cell Res.* **2001**, *267* (2), 173–183.
(20) Groves, J. T.; Mahal, L. K.; Bertozzi, C. R. *Langmuir* **2001**, *17* (17), 5129–5133.
(21) Yang, T.; Baryshnikova, O. K.; Mao, H.; Holden, M. A.; Cremer, P. S. *J. Am. Chem. Soc.* **2003**, *125* (16), 4779–4784.
(22) Nabika, H.; Sasaki, A.; Takimoto, B.; Sawai, Y.; He, S.; Murakoshi, K. *J. Am. Chem. Soc.* **2005**, *127* (48), 16786–16787.
(23) Howland, M. C.; Sapuri-Butti, A. R.; Dixit, S. S.; Dattelbaum, A. M.; Shreve, A. P.; Parikh, A. N. *J. Am. Chem. Soc.* **2005**, *127* (18), 6752–6765.
(24) Okazaki, T.; Inaba, T.; Tatsu, Y.; Tero, R.; Urisu, T.; Morigaki, K. *Langmuir* **2009**, *25* (1), 345–351.
(25) Okazaki, T.; Tatsu, Y.; Morigaki, K. *Langmuir* **2009**, *26* (6), 4126–4129.
(26) Morigaki, K.; Baumgart, T.; Jonas, U.; Offenhausser, A.; Knoll, W. *Langmuir* **2002**, *18* (10), 4082–4089.
(27) Morigaki, K.; Baumgart, T.; Offenhausser, A.; Knoll, W. *Angew. Chem., Int. Ed. Engl.* **2001**, *40* (1), 172–174.
(28) Groves, J. T.; Ulman, N.; Boxer, S. G. *Science* **1997**, *275* (5300), 651–653.
(29) Kung, L. A.; Kam, L.; Hovis, J. S.; Boxer, S. G. *Langmuir* **2000**, *16* (17), 6773–6776.
(30) Hovis, J. S.; Boxer, S. G. *Langmuir* **2000**, *16* (3), 894–897.
(31) Hovis, J. S.; Boxer, S. G. *Langmuir* **2001**, *17* (11), 3400–3405.
(32) Vogel, N.; Jung, M.; Retsch, M.; Knoll, W.; Jonas, U.; Köper, I. *Small* **2009**, *5* (7), 821–825.
(33) Smith, A. M.; Vinchurkar, M.; Gronbech-Jensen, N.; Parikh, A. N. *J. Am. Chem. Soc.* **2010**, *132* (27), 9320−9327.
(34) Nuzzo, R. G.; Allara, D. L. *J. Am. Chem. Soc.* **1983**, *105* (13), 4481–4483.
(35) Naumann, R.; Schiller, S. M.; Giess, F.; Grohe, B.; Hartman, K. B.; Kärcher, I.; Köper, I.; Lübben, J.; Vasilev, K.; Knoll, W. *Langmuir* **2003**, *19* (13), 5435–5443.
(36) Butt, H. J.; Wang, D. N.; Hansma, P. K.; Khlbrandt, W. *Ultramicroscopy* **1991**, *36* (4), 307–318.
(37) Hegner, M.; Wagner, P.; Semenza, G. *Surf. Sci.* **1993**, *291* (1−2), 39–46.
(38) Vogel, N.; Jung, M.; Bocchio, N. L.; Retsch, M.; Kreiter, M.; Köper, I. *Small* **2010**, *6* (1), 104–109.
(39) Retsch, M.; Zhou, Z.; Rivera, S.; Kappl, M.; Zhao, X. S.; Jonas, U.; Li, Q. *Macromol. Chem. Phys.* **2009**, *210*, 230.
(40) Baumgart, T.; Offenhauser, A. *Biophys. J.* **2002**, *83* (3), 1489–1500.
(41) Axelrod, D.; Koppel, D. E.; Schlessinger, J.; Elson, E.; Webb, W. W. *Biophys. J.* **1976**, *16* (9), 1055–1069.
(42) Soumpasis, D. M. *Biophys. J.* **1983**, *41* (1), 95–97.
(43) Vockenroth, I. K.; Rossi, C.; Shah, M. R.; Köper, I. *Biointerphases* **2009**, *4* (2), 19–26.
(44) Elbert, R.; Laschewsky, A.; Ringsdorf, H. *Abstr. Pap. Am. Chem. Soc.* **1985**, *189* (Apr), 139-POLY.
(45) Hub, H. H.; Hupfer, B.; Koch, H.; Ringsdorf, H. *Angew. Chem., Int. Ed. Engl.* **1980**, *19* (11), 938–940.
(46) Chi, L. F.; Anders, M.; Fuchs, H.; Johnston, R. R.; Ringsdorf, H. *Science* **1993**, *259* (5092), 213–216.
(47) Regen, S. L.; Czech, B.; Singh, A. *J. Am. Chem. Soc.* **1980**, *102* (21), 6638–6640.
(48) Ringsdorf, H.; Schlarb, B.; Venzmer, J. *Angew. Chem., Int. Ed. Engl.* **1988**, *27* (1), 113–158.
(49) Daly, S. M.; Heffernan, L. A.; Barger, W. R.; Shenoy, D. K. *Langmuir* **2006**, *22* (3), 1215–1222.
(50) Obrien, D. F.; Whitesides, T. H.; Klingbiel, R. T. *J. Polym. Sci., Part C: Polym. Lett.* **1981**, *19* (3), 95–101.
(51) Day, D.; Ringsdorf, H. *J. Polym. Sci., Part C: Polym. Lett.* **1978**, *16* (5), 205–210.
(52) Gupta, C. M.; Costello, C. E.; Khorana, H. G. *Proc. Natl. Acad. Sci. U.S. A.* **1979**, *76* (7), 3139–3143.
(53) Wegner, G. *Chimia* **1974**, *28* (9), 475–484.
(54) Vanderah, D. J.; Pham, C. P.; Springer, S. K.; Silin, V.; Meuse, C. W. *Langmuir* **2000**, *16* (16), 6527–6532.
(55) Carreon, M. D. P.; Burillo, G.; Fomina, L.; Ogawa, T. *Polym. J.* **1998**, *30* (2), 95–99.
(56) Day, D.; Hub, H. H.; Ringsdorf, H. *Isr. J. Chem.* **1979**, *18* (3−4), 325–329.
(57) Gaboriaud, F.; Volinsky, R.; Berman, A.; Jelinek, R. *J. Colloid Interface Sci.* **2005**, *287* (1), 191–197.
(58) Okada, S.; Peng, S.; Spevak, W.; Charych, D. *Acc. Chem. Res.* **1998**, *31* (5), 229–239.
(59) Sanii, B.; Parikh, A. N. *Biophys. J.* **2007**, 422A–422A.
(60) Kusumi, A.; Nakada, C.; Ritchie, K.; Murase, K.; Suzuki, K.; Murakoshi, H.; Kasai, R. S.; Kondo, J.; Fujiwara, T. *Annu. Rev. Biophys. Biomolec. Struct.* **2005**, *34* (1), 351–378.
(61) de Brabander, M.; Nuydens, R.; Ishihara, A.; Holifield, B.; Jacobson, K.; Geerts, H. *J. Cell Biol.* **1991**, *112* (1), 111–124.
(62) Dietrich, C.; Bagatolli, L. A.; Volovyk, Z. N.; Thompson, N. L.; Levi, M.; Jacobson, K.; Gratton, E. *Biophys. J.* **2001**, *80* (3), 1417−1428.
(63) Dietrich, C.; Volovyk, Z. N.; Levi, M.; Thompson, N. L.; Jacobson, K. *Proc. Natl. Acad. Sci. U.S.A.* **2001**, *98* (19), 10642–10647.
(64) Mcintyre, J. C.; Sleight, R. G. *Biochemistry* **1991**, *30* (51), 11819–11827.
(65) Hromada, L. P.; Nablo, B. J.; Kasianowicz, J. J.; Gaitan, M. A.; DeVoe, D. L. *Lab Chip* **2008**, *8* (4), 602–608.